Contribution from the Department of Chemistry,
Texas A&M University, College Station, Texas 77843-3255

Spin State Stabilities and Distortions of the Novel MN_3^{6-} (M = V, Cr, Fe) Ions

Kyeong Ae Yee and Timothy Hughbanks*

Received December 2, 1991

The electronic structures of the MN_3^{6-} (M = V, Cr, Fe) ions are examined with the intent of understanding their structures and spin states. The CrN_3^{6-} ion found in Ca_3CrN_3 has a unique low-spin electronic state, as judged by the magnetic properties reported by DiSalvo and co-workers. The ion's reported planar C_{2v} geometry is entirely consistent with a Jahn-Teller distortion that is expected on the basis of simple theory. Having adopted a Li_6MN_3 model to study these ions by use of ab initio methods, for both the Cr and Fe systems we find the D_{3h} quartet state that is most stable at the SCF level gives way to a C_{2v} doublet ground state with the inclusion of a modest degree of correlation (SD-CI). The diamagnetism and structure of the recently synthesized VN_3^{6-} ion is well accounted for in our treatment. Bond lengths for the optimized geometry of Li_6CrN_3 are found to be in good agreement with the reported C_{2v} structure in Ca_3CrN_3. In contrast, the D_{3h} geometry reported for the FeN_3^{6-} ion [in $(Ca_3N)_2[FeN_3]$ and Ba_3FeN_3] is at odds with an expected Jahn-Teller instability, if the FeN_3^{6-} ion has a low-spin doublet ground state as we predict. It is likely that the observed D_{3h} structure of FeN_3^{6-} ions are the result of dynamic Jahn-Teller effects or stabilization by interionic interactions.

Introduction, Simple Theory of MN_3^{6-} Ions

A number of newly synthesized metal nitrides exhibit unusual solid-state structures that suggest the presence of extensive chemical unsaturation and metal-nitrogen multiple bonding. Among these compounds are several in which quasimolecular ions have been identified. The series of 16 valence electron molecules that includes NO_2^+, CO_2, N_2O, N_3^-, and CN_2^{2-} has recently been augmented by the solid-state synthesis of the symmetrical BN_2^{3-} species, isolated in alkali metal salts $M^I_3BN_3$ (M^I = Li, Na). BN_2^{3-} has the expected short B-N bond length of 1.34 Å.[1-3] Even more remarkable additions to this molecular family are ZnN_2^{4-} and FeN_2^{4-}, respectively discovered in DiSalvo's and Kniep's laboratories.[4,5] These linear ions establish a connection to several low valent nitridoniccolates containing infinite chains with linearly coordinated metal centers: CaNiN,[6] BaNiN, and $Ba_8Ni_6N_7$.[7,8]

Ca_3CrN_3 is a quasimolecular material in which Ca^{2+} ions serve to stabilize the unusual CrN_3^{6-} ion.[9] The CrN_3^{6-} ions have C_{2v} symmetry, distorted from an ideal D_{3h} structure toward a T geometry (see the top of Figure 1). Magnetic susceptibility data indicate that the CrN_3^{6-} ion has a low-spin ($S = {}^1/_2$) electronic state that is unprecedented for Cr^{III}. The ion's shape is consistent with this and would be expected to distort in just the manner observed due to a Jahn-Teller instability for the D_{3h} geometry, as we discuss below.[10] While the CrN_3^{6-} ions would otherwise be expected to show *some* distortion since Ca_3CrN_3 crystallizes in an orthorhombic space group with the CrN_3^{6-} ions positioned on sites of C_{2v} symmetry, in the observed structure not only is the angle distortion substantial, the Cr-N bond length asymmetry is also that expected for a Jahn-Teller distortion.

The above remarks are supported explicitly by calculation. In Figure 1 is an orbital diagram showing the Cr d levels, derived from extended Hückel (EH) MO calculations for the D_{3h} and C_{2v} geometries. Focusing on the D_{3h} structure, we see that the lowest occupied d level is a s-d_{z^2} hybrid (a'_1) that is virtually Cr-N nonbonding. The s-d mixing in this MO serves to minimize the Cr-ligand overlap and the orbital's amplitude in the molecular plane. Because of this and the strong π donation of the nitride ligands, this orbital lies below the Cr-N π^* set (e''-d_{xz} and d_{yz}) that constitutes a doubly degenerate pair for the D_{3h} geometry. The highest-lying d levels have e' symmetry and are the $\{d_{x^2-y^2}, d_{xy}\}$ set, destabilized by both σ^* and π^* interactions with ligands in the molecular plane. For a low-spin configuration, the e'' levels hold only one electron between them, and the $^2E''$ symmetry ground state for the D_{3h} ion would be Jahn-Teller unstable. When the symmetry is lowered to C_{2v}, the e'' set breaks into b_1 and a_2; the b_1 orbital is symmetric with respect to reflection in the plane perpendicular to the molecular plane and becomes stabilized for the T distortion. Note that the Cr-N bond length asymmetry is a result of the π-bonding asymmetry in this singly occupied orbital. If CrN_3^{6-} had a *quartet* ground state as is usual for Cr^{III}, then the ground configuration would not be Jahn-Teller unstable, and we would expect the coordination environment to be more regular, with NCrN angles closer to 120° and less Cr-N bond length asymmetry.

Vennos and DiSalvo have recently synthesized an analogous vanadium-containing material, Ca_3VN_3, in which planar VN_3^{6-} ions with virtual C_{2v} symmetry can be identified.[11] The C_{2v} symmetry exhibited by VN_3^{6-} might appear to contradict the hypothesis that the departure from D_{3h} symmetry is due to a Jahn-Teller distortion, but there are important differences between these two systems that actually support our model. The d^2 VN_3^{6-} ion is diamagnetic, as we would expect if the a_1 (s-d_{z^2} hybrid) orbital lies lowest of the orbitals in the d-manifold. Also, though the larger of the NVN angles is opened up to 130°, to within experimental error the bond *lengths* are equal: 1.820 (6), 1.827 (7), 1.811 (6) Å. It seems reasonable to assume that the angular asymmetry is due to the exigencies of crystal packing.

Cordier and co-workers have reported the synthesis of Ca_6MN_5 materials (M = Fe, Ga) in which "isolated" MN_3^{6-} ions are found, surrounded only by Ca^{2+} ions.[12] This isotypic pair of compounds may be formulated as $(Ca_3N)_2[MN_3]$, where MN_3^{6-} ions are sandwiched between $^2_\infty[Ca_3N]^{3+}$ layers (with an anti-BiI_3 structure). In both compounds, MN_3^{6-} ions are reported to sit on high symmetry positions for which D_{3h} symmetry is crystallographically "imposed". The Fe-N distance is reported to be 1.770 (15) Å as compared with a Ga-N distance of 1.951 (28) Å in the gallium analogue. If we compare either the Fe^{III} low-spin six-coordinate radius with that for Ga^{III} (0.69 vs 0.76 Å, respectively) or four-coordinate radii (Fe^{III}, 0.63 Å; Ga^{III}, 0.61 Å),[13] we conclude that there is a large differential shortening of the Fe-N distances peculiar to these ions that indicates Fe-N π bonding is strong. As Figure 1 indicates, we calculate an even larger gap between the e'' and e' sets than we get for the a'_1-e'' gap for the D_{3h}

* To whom correspondence should be addressed.

(1) Yamane, H.; Kikkawa, S.; Horiuchi, H.; Koizumu, M. *J. Solid State Chem.* **1986**, *65*, 6.
(2) Yamane, H.; Kikkawa, S.; Koizumu, M. *J. Solid State Chem.* **1987**, *71*, 1.
(3) Evers, J.; Munsterkotter, M.; Oehlinger, G.; Polborn, K.; Sendlinger, B. *J. Less-Common Met.* **1990**, *162*, L17.
(4) Chern, M. Y.; DiSalvo, F. J. *J. Solid State Chem.* **1990**, *88*, 528.
(5) Gudat, A.; Kniep, R.; Rabenau, A. *Angew. Chem., Int. Ed. Engl.* **1991**, *30*, 199.
(6) Chern, M. Y.; DiSalvo, F. J. *J. Solid State Chem.* **1990**, *88*, 459.
(7) Gudat, A.; Haag, S.; Kniep, R.; Rabenau, A. *J. Less-Common Met.* **1990**, *159*, L29.
(8) Gudat, A.; Milius, W.; Haag, S.; Kniep, R.; Rabenau, A. *J. Less-Common Met.* **1991**, *168*, 305.
(9) Vennos, D. A.; Badding, M. E.; DiSalvo, F. J. *Inorg. Chem.* **1990**, *29*, 4059.
(10) Hughbanks, T. In *Inorganometallic Chemistry*; Fehlner, T., Ed.; Plenum Press: New York, 1992.
(11) Vennos, D. A.; DiSalvo, F. J. *J. Solid State Chem.* Submitted for publication.
(12) Cordier, G.; Höhn, P.; Kniep, R.; Rabenau, A. *Z. Anorg. Allg. Chem.* **1990**, *591*, 58.
(13) Shannon, R. D. *Acta Crystallogr.* **1976**, *A32*, 751.

0020-1669/92/1331-1921$03.00/0 © 1992 American Chemical Society

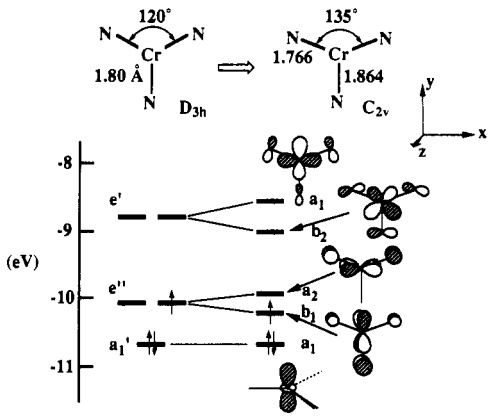

Figure 1. Molecular orbital diagram from an extended Hückel calculation on the CrN_3^{6-} ion for the D_{3h} and the observed C_{2v} geometry.

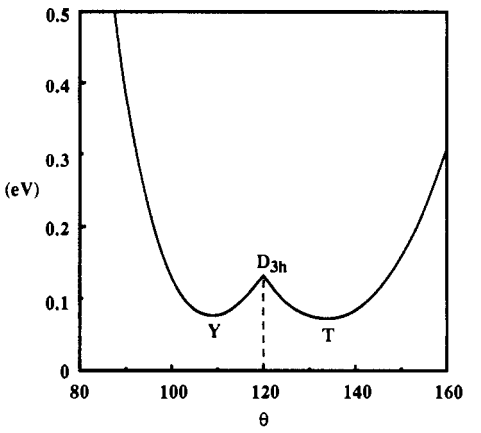

Figure 2. Potential energy surface curve of the d^3 CrN_3 system for angular distortion from the trigonal planar structure. Two minima have been denoted as T and Y.

geometry. Though magnetic measurements have not been reported for Ca_6FeN_5, it seems likely that the iron is low-spin on both structural and theoretical grounds. But then a $(a'_1)^2(e'')^3$ configuration is indicated and should also yield a Jahn–Teller unstable $^2E''$ ground state. By this line of reasoning, the FeN_3^{6-} ion would be expected to distort.

The available crystallographic data for Ca_6FeN_5 may not actually rule the distortion out because the poor quality of available crystals precluded a precise structure determination.[12] The nitrogen atom positions were refined only isotropically, and standard deviations in the thermal parameters were as large as the parameters themselves. However, the FeN_3^{6-} ion has also been found in $Ba_3[FeN_3]$, on a site with C_{3h} symmetry, and with an even shorter Fe–N bond length of 1.73 (1) Å.[14] In this instance the structure determination unambiguously indicates a trigonal-planar structure.

Some questions about these systems have now emerged. First, we wish to know the spin state of the FeN_3^{6-} ions in these materials. The structural results discussed in the preceding paragraphs are clearly contradictory; if this ion is low-spin, it would seem that it should not have D_{3h} symmetry, and if it is high-spin the Fe–N bond lengths would be expected to be longer. The observed low-spin state of CrN_3^{6-} ion is in accord with its C_{2v} structure, and it is tempting to expect FeN_3^{6-} ion to also be low-spin. One might argue that more of the antibonding orbitals of FeN_3^{6-} ion are occupied, which implies relatively longer Fe–N bonds, leading to weaker ligand field splittings and thus to a greater probability of a high-spin ground state. In what follows we present a more thorough investigation of geometrical particulars within the EH model; and to delve a bit deeper into this problem, we have used a $M(NLi_2)_3$ model for investigation with ab initio computational methods. We will present results for the vanadium, chromium, and iron systems, the first two serving as controls for evaluating the appropriateness of our treatment of the latter case where no magnetic data has been reported.

Spin States and Jahn–Teller Distortions

The Extended Hückel Model. In Figure 2 we show a potential energy surface for bending of the CrN_3^{6-} ion along a simple C_{2v}–D_{3h}–C_{2v} path, calculated using the extended Hückel method.[15,16] Only angular variations (changes in θ, see structure 1) were considered. The two minima expected on the basis of this

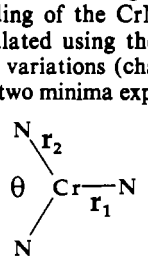

1

ion's Jahn–Teller instability are denoted as T and Y in reference to the molecule's shape at $\theta > 120°$ and $\theta < 120°$, respectively. The calculated minimum at the T geometry is for $\theta = 134°$ and at Y is for $\theta = 108°$, both being at virtually the same energy. Experimentally, the angle θ for CrN_3^{6-} ion in Ca_3CrN_3 is 135°. However, with this purely angular distortion, we find the Jahn–Teller stabilization to be quite small, only 1.4 kcal/mol below the D_{3h} geometry. The energy gained by splitting the degenerate e'' set is quickly compensated by N–N repulsions in the molecular plane.

The extended Hückel method is generally most useful for prediction of such angular distortions, and coupling this motion with a bond-stretching mode of the same symmetry is precarious. However, the small energy stabilization we see implies that angle-bending distortions are likely to be secondary to stretching distortions on the true Jahn–Teller surface. As the experimental data bear out, the N–M–N angles actually observed are probably more a function of the binding of nitrogens to surrounding alkaline earth centers than anything else.

Ab Initio Results. Basis sets used in our calculations are outlined in the Appendix. The MN_3^{6-} (M = V, Cr, Fe) ions have been modeled as Li_6MN_3 molecules, as illustrated in structure 2. The

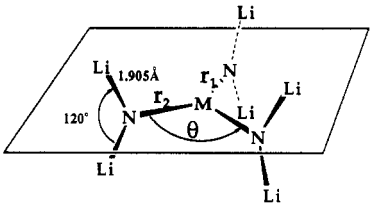

2

lithium centers are necessary to stabilize the electrostatic field of these highly charged ions. Our model is a reasonable representation of the surrounding alkaline earth cation environment in which the MN_3^{6-} ions are actually found. Two lithium atoms were fixed at a distance of 1.905 Å from each terminal nitrido and are symmetrically disposed above and below the CrN_3 plane. In all geometry optimizations, C_{2v} symmetry was imposed, and both the Li–N and Li–N–M angles were fixed so that all angles about the nitrogens were 120°. The distance between Li and N was chosen as an average of values found in a number of azole–Li^+ complexes.[17-19]

In Tables I and II, computed values for three variables (see structure 2) associated with optimized geometries are given in the third, fourth, and fifth columns, for Li_6CrN_3 and Li_6FeN_3, respectively. Energy differences between the D_{3h} and both the T and Y structures are shown in the final two columns, at electron

(14) Höhn, P.; Kniep, R.; Rabenau, A. *Z. Kristallogr.* **1991**, *196*, 153.
(15) Hoffmann, R.; Lipscomb, W. N. *J. Chem. Phys.* **1962**, *37*, 2872.
(16) Hoffmann, R. *J. Chem. Phys.* **1963**, *39*, 1397.
(17) Alcami, M.; Mo, O.; Yanez, M. *J. Phys. Chem.* **1989**, *93*, 3929.
(18) Patterman, S. P. *J. Am. Chem. Soc.* **1970**, *92*, 1150.
(19) Stucky, G. D. *Adv. Chem. Ser.* **1974**, *130*, 50.

Table I. Calculated Geometries, Energies, and Basis Sets for Li_6CrN_3

basis set[a]	variables	$^2B_1$ (T)	$^4A_2'$ (D_{3h})	$^2A_2$ (Y)	$\Delta E(^2B_1-^4A_2')$ HF/CI[b]	$\Delta E(^2A_1-^4A_2')$ HF/CI[b]
I	r_1	1.868	1.873	1.810		
	r_2	1.823	1.873	1.850	41.9/2.0	41.7/1.8
	θ	122.0	120	118.2		
II	r_1	1.870	1.877	1.805		
	r_2	1.817	1.877	1.851	39.0/−3.5	38.8/−3.5
	θ	123.2	120	117.0		
III	r_1	1.895	1.920	1.850		
	r_2	1.859	1.920	1.881	39.7/−4.1	39.6/−4.1
	θ	121.8	120	117.2		
IV	r_1	1.892	1.918	1.848		
	r_2	1.854	1.918	1.877	38.7/−6.0	38.6/−6.0
	θ	121.8	120	117.0		

[a] For all basis sets, Huzinaga's (43) fully contracted basis was used for Li. I, double-ζ + 4p polarization function for Cr, double-ζ for N; II, double-ζ + 4p polarization function and diffuse d for Cr, double-ζ for N; III, double-ζ + 4p polarization function for Cr, double-ζ + sp diffuse functions for N; IV, double-ζ + 4p polarization function and diffuse d for Cr, double-ζ + sp diffuse function for N. [b] Energy differences in kcal/mol.

Table II. Calculated Geometries, Energies, and Basis Sets for Li_6FeN_3

basis set[a]	variables	$^2A_2$ (T)	$^6A_1'$ (D_{3h})	$^2B_1$ (Y)	$\Delta E(^2A_2-^6A_1')$ HF/CI[b]	$\Delta E(^2B_1-^6A_1')$ HF/CI[b]
I	r_1	1.770	1.899	1.636		
	r_2	1.654	1.899	1.718	136.1/−2.1	136.4/−2.0
	θ	121.8	120	118.8		
II	r_1	1.770	1.903	1.637		
	r_2	1.655	1.903	1.718	137.1/−4.5	137.4/−4.5
	θ	122.0	120	118.6		

[a] For all basis sets, Huzinaga's (43) fully contracted basis was used for Li. Basis sets I and II are analogous to those for the Cr case (Table I). [b] Energy differences in kcal/mol.

correlated and uncorrelated levels of theory.

Let us first point out some general trends in these results. As expected on qualitative grounds, the average M–N bond lengths computed for all treatments indicate a shortening for the low-spin states; this trend is slightly intensified as basis set size increases. Energy differences between the T and Y optimized geometries of the low-spin states are negligible, regardless of the level of calculation. Also, though the low-spin states are always subject to a Jahn–Teller distortion, little of this is manifest in the deviation of the N–M–N angles from 120°. The expected importance of including correlation when evaluating relative spin state stability is underscored by these results for all basis sets; low-spin states were dramatically stabilized when CI calculations were performed. Coupled with the improvement in basis set, the inclusion of correlation yields a prediction that both the Cr and Fe systems should have doublet ground states with C_{2v} structures.

We have performed CI calculations only at single points using SCF-optimized geometries. Because our results show the low-spin states to be favored even with a modestly correlated wavefunction, we judged further computational effort to be unnecessary in answering the question of spin-state stability. Generally, spin-paired states continue to improve relative to spin-unpaired states when more extensive correlation calculations are performed. We expect greater changes in low-spin state geometries than in high-spin state geometries when we move from the SCF level to correlated treatments since wavefunctions for the high-spin states are better represented by single determinants. Thus, we assume that geometry optimization in conjunction with CI calculations shouldn't be necessary to establish the greater stability of the low-spin states, since the relative stability of low-spin states would only be further enhanced.

The chemical reasons underlying the preference for low-spin states are intuitively clear. Terminal nitrido groups are among the strongest of π donors, and only in low-spin states will the potential π bonding be maximally realized. Carter and Goddard reach similar conclusions in their GVB study of the $Cr(CH_2)^+$ ion.[20] Furthermore, π delocalization of the valence electrons reduces the electron–electron repulsions between them. Since the pairing of electrons in low-spin states is associated with greater electron–electron repulsion, molecules with greater orbital delocalization have a greater tendency to adopt low-spin states (assuming one compares cases with equal orbital energy splittings).[21]

Table III. SCF and SD–CI Energies[a] for Li_6CrN_3 for the Observed Geometry of CrN_3^{6-}

method[c]	$^2B_1$	$^4A_2'$	$\Delta E(^2B_1-^4A_2')$[b]
HF	−1249.67811	−1249.68034	1.4
CI	−1250.18767	−1250.16702	−13.0

[a] The total energies are in a.u. [b] kcal/mol. [c] Basis set IV (see Table I).

For CrN_3^{6-}, the biggest difference between the computed low-spin geometry and that observed in Ca_3CrN_3 is for the N–Cr–N angles. It isn't clear whether this represents a serious discrepancy, given that VN_3^{6-} exhibits nearly as great an angle distortion (θ = 130°) that is clearly *not* a result of a Jahn–Teller distortion (see below). The calculated differences in the two unique Cr–N bond lengths in Li_6CrN_3 fall into the range 0.04–0.05 Å, while that observed for Ca_3CrN_3 is 0.10 Å. This difference should not cause much concern given the fact that our geometry optimizations were carried out at the SCF level.

Our results for Li_6FeN_3 and their comparison with the Cr analogue strongly indicate that FeN_3^{6-} is a low-spin ion. While calculations at the SCF level favor a high-spin ground state, with the inclusion of correlation the low-spin doublet state(s) are found to be stable. The very large energy difference between the doublet and sextet found at the SCF level for Li_6FeN_3 (≈137 kcal/mol) is not as alarming as it may seem. In the Cr case the high-spin and low-spin states differ by the formation of one electron pair, and in the Fe case two electron pairs are involved. The introduction of correlation compensates for the uneven correlation of like-spin electrons that is characteristic of Hartree–Fock theory.

The average bond lengths calculated for the two states are an even more compelling indicator that the low-spin state does indeed prevail experimentally. In either the $^2A_2$(T) or the $^2B_1$(Y) states, the average Fe–N bond lengths are calculated to be in the range of 1.69 Å as opposed to the range of 1.90 Å found for the high-spin

(20) Carter, E. A.; Goddard, W. A., III *J. Phys. Chem.* **1984**, *88*, 1485.

(21) Simpson, C. Q., III; Hall, M. B.; Guest, M. F. *J. Am. Chem. Soc.* **1991**, *113*, 2898.

Table IV. Calculated Geometries, Energies, and Basis Sets for Li_6VN_3

basis set[a]	variables	$^3B_1$ (T)	$^1A_1'$ (D_{3h})	$^3A_2$ (Y)	$\Delta E(^1A_1'-^3A_2)$ HF/CI[b]	$\Delta E(^1A_1'-^3B_1)$ HF/CI[b]
I	r_1	1.936	1.852	1.855		
	r_2	1.873	1.852	1.913	13.8/−10.6	13.8/−10.7
	θ	123.2	120	117.2		
IV	r_1	1.982	1.861	1.910		
	r_2	1.924	1.861	1.961	9.2/−26.5	9.3/−26.6
	θ	123.8	120	115.8		

[a] For all basis sets, Huzinaga's (43) fully contracted basis was used for Li. Basis sets I and IV are analogous to those for the Cr case (Table I). [b] Energy differences in kcal/mol.

Table V. Parameters for EH Calculations

	orbital	H_{ii}, eV	ζ_1[a]	ζ_2[a]	c_1[b]	c_2[b]
Cr	3d	−11.20	4.95	1.80	0.5060	0.6750
	4s	−8.66	1.70			
	4p	−5.24	1.70			
N	2s	−26.0	1.95			
	2p	−13.4	1.95			

[a] Coefficients used in double-ζ expansion. [b] Slater-type orbital exponents.

$^6A'_1(D_{3h})$ state. The shorter values are in better agreement with the observed Fe–N distances of 1.77 Å in Ca_6FeN_5 or 1.73 Å in $Ba_3[FeN_3]$.[12,14] We believe that the observed Fe–N distances in these materials represent *average* Fe–N distances that are either crystallographically indistinguishable (because the distorted ions are orientationally disordered on high symmetry positions) or are dynamically interconverting (i.e., a dynamic Jahn–Teller effect is operative). The latter possibility seems especially likely given the fact that our calculated T and Y structures are close in energy. Though we have not attempted to calculate a potential energy surface that connects the two sets of three equivalent structures, it seems quite likely that barriers between the T and Y structures are small. One of these structures may be the transition state for interconversion between equivalent forms of the other. If so, trapping the FeN_3^{6-} ion in an environment with lower symmetry might be sufficient to induce a static distortion. Conversely, it may be that if the CrN_3^{6-} ion can be isolated in an otherwise 3-fold symmetric environment, a dynamic Jahn–Teller effect will be observed.

As a test of whether the angular distortion observed in Ca_3CrN_3 might influence the relative spin state stabilities, calculations were carried out at the experimental geometry for this system (r_1 = 1.864 Å, r_2 = 1.766 Å, θ = 134.8°; see Table III). As expected, the quartet state is more destabilized by moving from its calculated minimum to the experimental geometry than is the $^2B_1$ state. This simply reflects the fact that there is a greater difference between the experimental geometry and the SCF minimum of the $^4A'_2$ state than the SCF minimum of the $^2B_1$ state. This effect is not as pronounced at the SD–CI level, but the quartet–doublet difference is still larger than is found at the SCF minima.

Finally, we turn our attention to the d^2 VN_3^{6-} ion, for which the geometrical roles of the low-spin and high-spin states are transposed. Referring to the orbital picture of Figure 1, we expect that in the spin-paired $(a'_1)^2$ configuration ($^1A'_1$ state) the ion will adopt a D_{3h} structure, and the high-spin states will be Jahn–Teller unstable. The data in Table IV show that the $^1A'_1$ (D_{3h}) state is clearly predicted to be the ground state, in agreement with the observed magnetic behavior of Ca_3VN_3.[11] As we have found for all the low-spin states, the observed M–N bond lengths (average, 1.82 Å) are in good agreement with those calculated even at the SCF level, and the calculated triplet-state bond lengths compared more poorly. We confidently attribute the observed angular distortions to be due to the (predominantly ionic) lattice energetics of Ca_3VN_3.

Concluding Remarks

Our study of MN_3^{6-}-based compounds (M = V, Cr, Fe) indicates that all contain low-spin ions and that the Cr- and Fe-containing species will display Jahn–Teller distortions. While this conclusion is in reasonable accord with available structural and magnetic data for the vanadium and chromium nitrides, it is at odds with the reported structures of the iron nitrides. This discrepancy may arise from unavoidable structural disorder or a dynamic Jahn–Teller effect in these materials and may only be settled if the FeN_3^{6-} ion can be isolated in an environment where significant bond length asymmetry can be unambiguously observed. Magnetic measurements of FeN_3^{6-}-containing compounds should be illuminating as well, particularly at low temperatures for $Ba_3[FeN_3]$. Besides deciding between low-spin and high-spin states, observed orbital contributions to the magnetic moments may distinguish between a D_{3h} geometry (where orbital contributions to the magnetism should appear as a first-order effect) and a distorted C_{2v} geometry (where orbital contributions to the moment will tend to be quenched in the ground state).

We do not know whether the interionic coupling that leads to antiferromagnetic ordering (at ~240 K) in Ca_3CrN_3 is also strong enough to quench the Jahn–Teller distortions in compounds like Ca_6FeN_5 or $Ba_3[FeN_3]$. Such a scenario is plausible; analogous Peierls distortions are predicted for the $^1_\infty[CoC^{3-}]$ chains in YCoC if they are low-spin[22] (or $^1_\infty[NiN^{2-}]$ chains in the isotypic CaNiN), but distortions are not observed.[6,23] Hoffmann and co-workers suggested that YCoC is instead a high-spin material.[22] A recent treatment of CaNiN using density functional theory nicely shows how a Peierls distortion in that system is suppressed by interactions between the $^1_\infty[NiN^{2-}]$ chains.[24]

As always, synthetic progress should be most interesting. If low-spin states continue to prevail in the MN_3^{6-} series (as we suspect), then MnN_3^{6-} will be a symmetrical d^4 ion with a triplet ground state and CoN_3^{6-} will also be symmetrical with a singlet ground state. Related oxides already exist, planar CoO_3^{4-} is found in $RbNa_7[CoO_3]_2$ and nearly planar FeO_3^{4-} in $Na_4[FeO_3]$.[25,26] If the general orbital ordering displayed in Figure 1 remains appropriate, then the d^6 FeO_3^{4-} ion should be stable in a D_{3h} geometry whether it is high-spin or low-spin. The experimental situation is structurally similar to that of VN_3^{6-}: the Fe–O distances are nearly equal (1.86, 1.87, and 1.89 Å), but the O–Fe–O angles show a larger spread (108°, 124°, and 126°). The d^7 ion CoO_3^{4-} should be subject to Jahn–Teller instability whether it is high- or low-spin, and the observed bond-length asymmetry is much more pronounced (distances: Co–O_1 = 1.91 Å, Co–O_2 = 1.83 Å, Co–O_3 = 1.83 Å; angles: O_1–Co–O_2 ≅ O_1–Co–O_3 = 111.5°, O_2–Co–O_3 ≅ 130°). Magnetic properties of these materials should also be informative.

Acknowledgment. Partial support of this research was derived from a grant (No. 010366-111) by the Texas Advanced Research Program. We also acknowledge the National Science Foundation for its support through a Presidential Young Investigator Award (Grant DMR-8858151) and the Robert A. Welch Foundation for its support through Grant A-1132. Thanks are extended to Prof. Michael Hall, Dr. Preston MacDougall, and Dr. Zhenyang Lin for assistance in carrying forward ab initio calculations. We thank Deborah Vennos and Prof. Frank DiSalvo for providing results prior to publication.

(22) Hoffmann, R.; Li, J.; Wheeler, R. *J. Am. Chem. Soc.* **1987**, *109*, 6600.
(23) Gerss, M. H.; Jeitschko, W. *Z. Naturforsch.* **1986**, *41B*, 946.
(24) Massida, S.; Pickett, W. E.; Posternak, M. *Phys. Rev. B* **1991**, *44*, 1258.
(25) Birx, J.; Hoppe, R. *Z. Anorg. Allg. Chem.* **1990**, *588*, 7.
(26) Rieck, H.; Hoppe, R. *Z. Anorg. Allg. Chem.* **1977**, *437*, 95.

Appendix

The extended Hückel method was used for calculations reported in Figures 1 and 2, parameters appear in Table V.

Ab initio MO calculations were performed using both the closed- and open-shell Hartree–Fock–Roothaan (HFR) methods.[27,28] All calculations were performed with the GAMESS package[29] on the Department of Chemistry FPS/UNIX 500EA computer. Ab initio calculations were carried out with several different basis sets, all derived from those of Huzinaga.[30] For the transition metals, double-ζ basis sets were derived from fully contracted (4333/43/4) primitive sets by splitting off the outermost primitive function in each case. 4p polarization functions are added for all the transition metals. For N a double-ζ basis was derived from Huzinaga's contracted (43/4) primitive set. The transition metal triple-ζ d basis sets were formed by augmentation with exponents one-third that of the most diffuse primitive. Nitrogen s–p diffuse functions were added as prescribed by Clark and co-workers.[31] For Li a fully contracted (43) primitive set was used. In the configuration–interaction calculations [all single- and double-excitations (SD–CI)], SCF optimization results were used as starting solutions. Unfortunately, convergence difficulties prevented us from carrying forward calculations for the two largest basis sets on $Fe(NLi_2)_3$. However, results for $Fe(NLi_2)_3$ obtained for the smaller basis sets are well in line with results obtained for the V and Cr analogues.

(27) Roothaan, C. C. *Rev. Mod. Phys.* **1951**, *23*, 69.
(28) Roothaan, C. C. *Rev. Mod. Phys.* **1960**, *32*, 179.
(29) Guest, M. F., SERC Darebury Laboratory, Warrington, WA4 4AD U.K.
(30) *Gaussian Basis Sets for Molecular Calculations*; Huzinaga, S., Ed.; Elsevier: Amsterdam, 1984.
(31) Clark, T.; Chandrasekhar, J.; Spitznagel, G. W.; Schleyer, P. V. R. *J. Comput. Chem.* **1983**, *4*, 294.

Contribution from Ames Laboratory and the Department of Chemistry, Iowa State University, Ames, Iowa 50011

Kinetics of Oxidation of Vanadium(IV) by Alkyl Hydroperoxides in Acidic, Aqueous Solution

Rong Ma, Andreja Bakac,* and James H. Espenson*

Received June 16, 1991

The title reactions produce VO_2^+ and products derived from β-scission of alkoxy radicals, largely acetone, ethane, and methane (*tert*-butyl hydroperoxide) or ethane, ethylene, and *n*-butane (*tert*-amyl hydroperoxide). The minor amounts of methane from the first reaction and the excess amount of ethane from the second suggest a small contribution from the oxidation of VO^{2+} by $^{\bullet}CH_3$ and $^{\bullet}C_2H_5$, respectively. The kinetic dependence of the main reaction upon $[H^+]$ is consistent with the formation of an intermediate $OVOOR^+$ present at steady-state concentrations. This intermediate produces VO_2^+ and $RO^{\bullet}$ in a rate-limiting step. The yield of VO_2^+ is stoichiometric in the *t*-AmOOH reaction, whereas only about half this amount of VO_2^+ is produced from *t*-BuOOH. Although chloride ions affect neither reaction, Br^- changes the stoichiometry, products, and kinetics of the *t*-BuOOH reaction, but not those of the *t*-AmOOH reaction. These differences are accounted for by the relative reactivities of the intermediate alkoxy radicals, $RO^{\bullet}$, toward β-scission versus bromide oxidation. Addition of alcohols with α-H's (i.e., CH_3OH, C_2H_5OH, $(CH_3)_2CHOH$) does not affect VO_2^+ production from *t*-AmOOH but does prevent VO_2^+ formation from *t*-BuOOH because VO_2^+ is reduced by the alcohol radical formed in the reaction between *t*-$BuO^{\bullet}$ and ROH. Several models are suggested, all of which feature β-scission of *t*-$BuO^{\bullet}$ and *t*-$AmO^{\bullet}$. The data pertaining to products and stoichiometry suggest an interaction or complexation of VO_2^+ by *t*-BuOOH (but not *t*-AmOOH), which is supported by product yields, ion-exchange isolation, and spectroscopic evidence.

Introduction

The reduction of peroxides by transition metal complexes is important in many contexts. This includes reactions that occur in biological systems and also certain metal-catalyzed oxidations. Vanadium toxicity may arise because of hydroxyl radicals formed in the reaction of vanadyl ions and hydrogen peroxide, which derives from superoxide reduction or disproportionation. Results have been reported concerning vanadate-dependent NADH oxidase present in cardiac cell membranes,[1] and both enzymatic[2-4] and nonenzymatic[4,5] oxidations by free-radical chains[6-8] have been identified. That hydroxyl radicals are produced[9] in the VO^{2+}–H_2O_2 reaction has been shown by spin-trapping and ESR detection.[10]

Also, reactions of peroxides are of importance in the context of oxygen activation.[11] Particular importance attaches to the *t*-BuOOH–$V^{IV}O$ system, the latter usually as $VO(acac)_2$. Epoxidation of alkenes is a fundamental and important reaction.[11,12] Vanadium-catalyzed selective peroxidation of olefins by alkyl hydroperoxides has become an important process for the manufacture of propylene oxide.[13,14] There has been no study of the kinetics of the VO^{2+}–*t*-BuOOH reaction, however, despite its importance, although it seems likely that free-radical intermediates are involved.

Peroxide reductions by metal ions continue to be of wide interest and are known to adopt a variety of mechanisms.[15] Among those one has to consider in the general case is the possibility of a group-transfer reaction that is, in effect, a two-electron process:

(1) Erdman, E.; Krawietz, W.; Philipp, G.; Hackbarth, I.; Schmitz, W.; Scholz, H.; Crane, F. L. *Nature* **1979**, *282*, 335.
(2) Ramasarma, T.; MacKellar, W. C.; Crane, F. L. *Biochim. Biophys. Acta* **1981**, *646*, 88.
(3) Briskin, D. P.; Thornley, W. R.; Poole, R. J. *Arch. Biochem. Biophys.* **1985**, *236*, 228.
(4) Coulombe, R. A., Jr.; Briskin, D. P.; Keller, R. J.; Thornley, W. R.; Sharma, R. P. *Arch. Biochem. Biophys.* **1987**, *255*, 267.
(5) Vyskocil, F.; Teisinger, J.; Dlouha, H. *Nature* **1980**, *286*, 516.
(6) Darr, D.; Fridovich, I. *Arch. Biochem. Biophys.* **1985**, *243*, 220.
(7) Darr, D.; Fridovich, I. *Arch. Biochem. Biophys.* **1984**, *232*, 562.
(8) Liochev, S.; Fridovich, I. *J. Free Radicals Biol. Med.* **1986**, *250*, 139.
(9) Keller, R. J.; Coulombe, R. A., Jr.; Sharma, R. P.; Grover, T. A.; Piette, L. H. *Free Radical Biol. Med.* **1989**, *6*, 15.
(10) Ozawa, T.; Hanaki, A. *Chem. Pharm. Bull.* **1989**, *37*, 1407.
(11) Sheldon, R. A.; Kochi, J. K. *Metal-Catalyzed Oxidations of Organic Compounds*; Academic Press: New York, 1981; Chapter 9.
(12) Jorgensen, K. A. *Chem. Rev.* **1989**, *89*, 431.
(13) Nishida, Y.; Yamada, K. *Inorg. Chim. Acta* **1990**, *174*, 1.
(14) Mimoun, H.; Mignard, M.; Brechot, P.; Scussine, L. *J. Am. Chem. Soc.* **1986**, *108*, 3711.
(15) Masarwa, M.; Cohen, H.; Meyerstein, D.; Hickman, D. L.; Bakac, A.; Espenson, J. H. *J. Am. Chem. Soc.* **1988**, *110*, 4293.

0020-1669/92/1331-1925$03.00/0 © 1992 American Chemical Society